Rational Design of β-sheet Peptides with Self-Assembly into Nanofibres on Remineralisation of Initial Caries Lesions

Zhong Cheng LI[1#], Xi QIN[1,2#], Qian REN[1], Die HU[1], Tian TIAN[1], Ting HE[1], Wei LI[1], Ling Lin ZHANG[1]

Objective: *To explore the self-assembly and gelation properties of synthetic peptides, and their efficacy on hydroxyapatite (HAP) nucleation and in situ remineralisation of initial caries lesions.*

Methods: *Mass spectrometry and reversed-phase high performance liquid chromatography (RPHPLC) were used to confirm the successful synthesis of peptides. Their self-assembly properties and conformation stability were evaluated using circular dichroism (CD) spectroscopy and Fourier-transform infrared spectroscopy (FTIR). Cell Counting Kit-8 (CCK-8; Dojindo, Kumamoto, Japan) was used to evaluate their cytotoxicity. The efficacy of the peptides on HAP nucleation and in situ remineralisation of initial caries lesions was explored using FTIR, scanning electron microscopy (SEM), transmission electron microscopy (TEM), X-ray diffraction and transverse microradiography analysis.*

Results: *Two kinds of self-assembly β-sheet peptides named ID4 and ID8, respectively, were successfully synthesised with purities greater than 95%. Both were stable under neutral physiological conditions and had low cytotoxicity. ID4 and ID8 showed calcium responsive self-assembly properties and could self-assemble into nanofibres. Compared with ID4, ID8 resulted in the rapid formation of hydrogel with a lower concentration of calcium, and self-assembled ID8 hydrogel induced the formation of flower-like HAP and significantly promoted the remineralisation of initial enamel caries.*

Conclusion: *ID8 could serve as the template to induce HAP nucleation and promote biomimetic remineralisation of initial caries lesions. These results underpin future research on peptide design, and ID8 may be a promising bioactive component for anti-caries applications.*

Key words: *β-sheet peptide, hydroxyapatite, initial caries lesions, remineralisation, self-assembly*

Chin J Dent Res 2020;23(2):131–141; doi: doi: 10.3290/j.cjdr.a44749

1 State Key Laboratory of Oral Diseases, National Clinical Research Centre for Oral Diseases, Department of Cariology and Endodontics, West China Hospital of Stomatology, Sichuan University, Chengdu, Sichuan Province, P.R. China.

2 Department of Oral Medicine, Shenzhen Stomatology Hospital, Shenzhen, Guangdong Province, P.R. China.

# These authors contributed equally to this work.

Corresponding author: Prof Ling Lin ZHANG, Department of Cariology and Endodontics, West China Hospital of Stomatology, No.14, 3rd Section, Renmin South Road, Sichuan University, Chengdu 610041, P.R. China. Tel: 86-28-85503470. Email: zhll_sc@163.com.

This research was supported by the National Natural Science Foundation of China (No. 81970931 to Ling Lin ZHANG).

Mature enamel is an acellular tissue which cannot self-repair once it is damaged by dental caries. In general, dental caries is a chronic progressive bacterial infection which occurs due to remineralisation and demineralisation becoming imbalanced, leading to a net loss of tooth minerals[1]. Therefore, promoting the remineralisation of initial caries lesions before they become cavities is an alternative restorative strategy against dental caries[2]. Recently, significant efforts have been made to promote remineralisation or inhibit the demineralisation of initial enamel caries using synthetic peptides under physiological conditions[3-8]. It is obvious that the in situ remineralisation of initial caries lesions using

synthetic peptides under physiological conditions is a desirable alternative restorative pathway against dental caries.

In general, self-assembly β-sheet peptide is recognised as a good template for hydroxyapatite (HAP) nucleation[9]. Enamel biomineralisation is highly orchestrated by ameloblasts and enamel matrix proteins (EMPs)[10]. Various proteins take part in this complicated process, with amelogenin being the most abundant. Amelogenin spontaneously self-assembles into hydrophobic nanospheres with supermolecular structures during enamel formation. These self-assembling hydrophobic nanospheres have been proposed to act as a structural framework related to HAP nucleation and growth[11,12]. Another major acidic protein in EMPs, enamelin, has been shown to self-assemble into β-sheet structure during enamel formation. Moreover, dentine phosphoprotein (DPP) is a major non-collagenous extracellular matrix protein in dentine, and self-assembles into a β-sheet–like conformation in the presence of Ca^{2+}, serving as a highly negatively charged surface. This surface may not only interact with the growing HAP crystals, but also be involved in the first crystal deposition during dentinogenesis. In addition, many in vitro experiments have confirmed the effect of self-assembly β-sheet structure on HAP nucleation[5,13-17]. Dentine matrix protein-1 (DMP-1) is an acidic non-collagenous protein that is necessary for the proper biomineralisation of dentine. He et al[18] demonstrated that intermolecular assembly of acidic clusters into a β-sheet template in DMP-1 was essential for HAP nucleation. Segman-Magidovich et al[9] observed that acidic β-sheet peptide P_{FD}-5 (13 amino acid residues) could induce adsorption and in situ nucleation of amorphous calcium phosphate in 1.5 times simulated body fluid (SBF). Stendahl et al[19] constructed an amphiphilic lipopeptide PA (peptide amphiphile) (11 amino acid residues and a long alkyl tail) and the peptide PA self-assembled into β-sheet nanofibre and attracted calcium and phosphorus in solution, thus promoting HAP nucleation and growth. These studies demonstrated that self-assembly β-sheet peptides are ideal templates for HAP nucleation.

Synthetic peptides can now be programmed to self-assemble into predefined conformations and nanostructures, which have been widely applied to biomimetic mineralisation of bone and teeth[20,21]. Ionic self-complementarity is a well-known structural motif of self-assembly β-sheet peptide design. However, classic ionic self-complementary self-assembly β-sheet peptides usually employed long sequence patterns and were not stable enough under physiological conditions[22]. Therefore, rational design of self-assembly β-sheet peptides with better stability under physiological conditions may be a promising biomimetic approach to treating initial caries lesions. In this study, the β-sheet peptides with shorter and optimised sequence patterns were designed rationally based on the $(XZXZ)_n$ sequence template, where X represented nonpolar amino acid, Z represented polar amino acid and n represented the number of repeats. Isoleucine was chosen as the hydrophobic amino acid residue (X) and aspartic acid was chosen as the hydrophilic amino acid residue (Z), the number of repeats was 1 and 2, and the acetyl group was added to the carboxyl end of the peptide to enhance its stability. Thus, the peptides Ac-Ile-Asp-Ile-Asp denoted as ID4 and Ac-Ile-Asp-Ile-Asp-Ile-Asp-Ile-Asp denoted as ID8 were designed and synthesised in this study.

The aim of this study was to design and synthesise self-assembly β-sheet peptides ID4 and ID8 with optimised short sequence patterns and to explore their self-assembly and gelation properties, and to investigate their stability under neutral physiological conditions. Finally, their effects on HAP nucleation and potential for in situ remineralisation of initial caries lesions were identified in vitro. We expected this study to offer a promising biomimetic agent for anti-caries application.

Materials and methods

Peptide synthesis and purification

The peptides ID4 (Ac-Ile-Asp-Ile-Asp) and ID8 (Ac-Ile-Asp-Ile-Asp-Ile-Asp-Ile-Asp) were synthesised by GL Biochem (Shanghai, China) using a standard fluorenylmethoxycarbonyl (Fmoc) solid-phase method. The synthesised peptides were then purified (> 95%) by reversed-phase high performance liquid chromatography (RPHPLC; CHTH Sci and Tech, Beijing, China). The peptide sequences and integrity were confirmed by electrospray ionisation mass spectrometry (ESI-MS; Shimadzu, Kyoto, Japan) as described previously[2]. The peptide powder was stored at −20°C.

Circular dichroism spectroscopy

Circular dichroism (CD) spectra were gathered over the range of 190–250 nm at room temperature using a CD spectropolarimeter (Chirascan, Applied Photophysics, Surrey, UK). The peptides ID4 and ID8 were diluted with deionised water (DIW) to 200 μM. The pH of the solution and whether it contained calcium were selected as two environmental conditions of peptide self-assembly. For

the pH condition, the pH of the ID4 and ID8 solutions was adjusted to 4.0, 5.0, 6.0 and 7.0 using hydrochloric acid (HCl) or ammonia. For the calcium condition, the peptide solutions were prepared in the absence and presence of calcium (1.5 mM $CaCl_2$). The measurements were conducted after 24 hours of incubation at 37°C. All spectra were obtained using a 0.5-mm bandwidth and a 100-nm/min scanning rate. CD spectroscopic data were analysed using CD Pro (JASCO, Tokyo, Japan) with CONTINLL as described previously[2].

Cytotoxicity assay

The effects of ID4 and ID8 on cell proliferation were investigated by a Cell Counting Kit-8 (CCK-8; Dojindo, Kumamoto, Japan) assay. Human oral keratinocyte (HOK) cells obtained from the American TypeCulture Collection (ATCC, 11303) were seeded at 2×10^3 cells per well in 96-well plates and incubated in Dulbecco's Modified Eagle Medium (DMEM; HyClone, Logan, UT, USA) with 10% foetal bovine serum (Gibco, Grand Island, NY, USA) (100 µl per well) for 24 hours, as described previously. Cells were exposed to ID4 and ID8 with the final concentrations of 0.625, 1.25, 2.5, 5 and 10 mg/ml. The cell viability was assessed after 24 hours of exposure. Absorbance at 450 nm was measured using Thermo Scientific Varioskan Flash (Thermo Fisher Scientific, Waltham, MA, USA). The absorbance was the average value measured from 5 wells in parallel for each concentration as described previously[2].

Gelation properties of ID4 and ID8

ID4 and ID8 were dissolved in NaOH solution to 10 mg/ml. For the pH condition, the pH of peptide solutions was adjusted to 4.0 using HCl or ammonia to trigger gelation according to the results of the above experiment. For the calcium condition, the alkalinity of the peptide solutions was adjusted to neutral (pH 7.0) using HCl. Different amounts of 1 M calcium solution (50 µl, 100 µl and 200 µl) were added to the peptide solutions to trigger gelation. Self-supporting hydrogels diluted with DIW were lyophilised for further characterisation.

Characterisation of ID4 and ID8 hydrogels

The lyophilised ID4 and ID8 hydrogel powders were mixed with potassium bromide (KBr) to a mass ratio of 1:20 and then milled and pressed into a transparent film for Fourier-transform infrared spectroscopy (FTIR). Infrared spectra in the 400–4000 cm^{-1} wavenumber range with a resolution of 2 cm^{-1} were obtained using a Nicolet 6700 spectrometer (Thermo Fisher Scientific, Waltham, MA, USA).

The lyophilised ID4 and ID8 hydrogels were also characterised by scanning electron microscopy (SEM) and transmission electron microscopy (TEM) with selected area electron diffraction (SAED). SEM images were obtained using a scanning electron microscope (Inspect F, FEI, Eindhoven, The Netherlands) at 20.0 kV. In TEM analysis, the lyophilised hydrogel powder dispersed with ethanol was observed using a Tecnai F20 S-TWIN electron microscope (FEI) at 120 kV.

HAP nucleation regulated by ID4 and ID8 hydrogels

The ID4 and ID8 hydrogels were incubated in 1.5 times SBF (120 mM NaCl, 22 mM $NaHCO_3$, 3.75 mM $CaCl_2$, 1.67 mM Na_2HPO_4, pH 7.4) for 1, 4 and 7 days at 37°C. The 1.5 times SBF was freshly prepared daily. The mineralised hydrogel was washed three times with DIW and then lyophilised for further characterisation.

The mineralised hydrogel was characterised by SEM (Inspect F, FEI, Eindhoven, The Netherlands), TEM-SAED (FEI Tecnai F20 S-TWIN) and X-ray diffraction (XRD) (Empyrean; PANalytical, Almelo, The Netherlands) with Cu Kα radiation (λ = 1.54 Å) operating at 40 kV and 40 mA, a sampling step of 0.026 and a 2θ range of 10–60°. In SEM analysis, the mineralised hydrogels at 1, 4 and 7 days were sputter-coated with gold for 30 seconds and then observed by SEM at an accelerating voltage of 20 keV.

Remineralisation efficacy of ID4 and ID8 hydrogels on initial caries lesions

Newly extracted bovine permanent incisors were chosen as substitutes for human teeth. The teeth were stored in DIW with a 0.5% thymol solution until required. The crowns of the bovine incisors were separated from the roots to make enamel samples as described previously[2]. The baseline surface microhardness (SMH_0) of the prepared samples was measured at five positions using a microhardness tester (Duramin-1/-2; Struers, Copenhagen, Denmark) and a Knoop indenter (Duramin-1/-2; Struers) with a load of 50 g for 15 seconds. Samples with Knoop hardness numbers (KNH) between 330 and 370 were selected for further study. Enamel blocks were submerged in the demineralisation solution (pH 4.5) containing 50 mM acetic acid, 2.2 mM $Ca(NO_3)_2$, 2.2 mM KH_2PO_4, 5.0 mM NaN_3, and 0.5 ppm NaF at 37°C for 3 days under continuous, low-speed magnetic stirring (100 rpm). Post-demineralisation surface microhardness (SMH_1) was measured as described above. Sixty enamel

blocks with SMH_1 between 130 and 225 KHN were selected for the subsequent remineralisation assay. The exposed windows on these samples were sealed with a film (4 × 2 mm), or an exposed area of 4 × 2 mm was left unsealed.

After demineralisation, all 60 enamel samples were randomly divided into 4 groups and treated with agents. The positive control group was treated with 1000 ppm NaF; the experimental groups were treated with 0.02 cm^3 10 mg/ml ID4 hydrogel or 0.02 cm^3 10 mg/ml ID8 hydrogel; and the negative control group was treated with DIW. Each sample was exposed to its respective solution for 30 minutes at room temperature and then rinsed three times with DIW, followed by immersion in artificial saliva at 37°C for 7 days. The artificial saliva containing 1.5 mM $CaCl_2$, 0.9 mM KH_2PO_4, 130 mM KCl, 1 mM NaN_3 and 20 mM HEPES (pH 7.0) was freshly prepared each day.

The SMH of each sample was measured again after remineralisation for 7 days (SMH_2) using five new indentations located close to those used to measure SMH_0 and SMH_1 while at least 100 μM away from them. After a load of 50 g for 15 seconds, there will be indentations on the surface of the sample, and the higher the KNH of the sample, the smaller the indentation area. The microhardness of the samples was obtained by measuring and calculating the pit area using the software of the microhardness tester. The percentage of surface microhardness recovery (SMHR%) for the nine groups was calculated as $SMHR\% = (SMH_2 - SMH_1)/(SMH_1 - SMH_0) \times 100\%$.

The enamel surfaces before etching, after etching and after remineralisation were all analysed using XRD by scanning the tooth slices directly. The reflection mode XRD with Cu Kα radiation (λ = 1.54 Å) operating at 40 kV and 40 mA with a sampling step of 0.026 and 2θ of range 10°–60° was used to analyse the enamel surfaces. The results were analysed using MDI Jade 5.0.

After remineralisation, the windows of the samples were cut into 300 μm–thick slices using a diamond-coated band saw (Struers) and then polished to about 100 μm. Each slice was then cleaned by 5 minutes of sonication (Jiahui, Suzhou, China) to remove any dust particles. The slices were fixed on Plexiglas sheet in a transverse microradiography (TMR) sample holder (Inspektor Research Systems BV, Amsterdam, The Netherlands) and microradiographs were taken alongside an aluminium calibration step wedge with 14 steps using a monochromatic CuK X-ray source (Philips, Eindhoven, The Netherlands) operated at 20 kV and 20 mA for an exposure time of 25 seconds as described previously[2]. Mineral loss, lesion depth and mineral content in different enamel layers were assessed using TMR software 2006 (Inspektor Research Systems). Therefore, ten TMR traces along each slice were measured, including five exposed areas and five not exposed areas.

Results

Characterisation of the synthesised peptides

RP-HPLC analysis showed that the elution times of ID4 and ID8 were 13.607 minutes and 9.33 minutes respectively with purities greater than 95%. Moreover, the mass spectra results showed strong peaks at the theoretical molecular weights of ID4 and ID8 (data not shown). These results confirmed the successful synthesis of ID4 and ID8.

As shown in Figs 1a to 1d, for the pH condition, ID4 was unstructured and showed no significant changes at pH 4.0, 5.0, 6.0 and 7.0. ID8 was unstructured at pH 5.0, 6.0 and 7.0, and self-assembled into β-sheet structure at pH 4.0. For the calcium condition, the percentage of β-sheet in ID4 increased to 52.6% from 20.3% in the presence of Ca^{2+} under a neutral pH environment, and ID8 contained a total of 99.63% β-sheet structure in the presence of Ca^{2+}.

Effect of ID4 and ID8 on cell viability

After a 30-minute treatment, the effect of ID4 and ID8 on cell viability showed no significant difference with the negative control group (Figs 2a and 2b).

Gelation properties of ID4 and ID8

The addition of 100 μl $CaCl_2$ (1 M) induced the formation of transparent ID8 hydrogel after 20 minutes, while ID4 required 200 μl $CaCl_2$.

In the FTIR results (Figs 2c and 2d), the peaks at 1631cm^{-1} (ID4) and 1633cm^{-1} (ID8) belong to the amide I band while the peaks at 1565 cm^{-1} (ID4) and 1558 cm^{-1} belong to the amide II band. These peaks confirmed the β-sheet structure of ID4 and ID8.

SEM images (Figs 3a to 3f) showed that ID4 and ID8 hydrogel self-assembled into nanofibres, and these nanofibres interweaved to form membrane-like structures. TEM images (Figs 4a to 4d) showed that the diameter of ID4 nanofibres was about 20 nm with a length between 0.4 and 0.6 μm, and ID8 nanofibres were about 50 nm in diameter with a length between 0.8 and 1.2 μm.

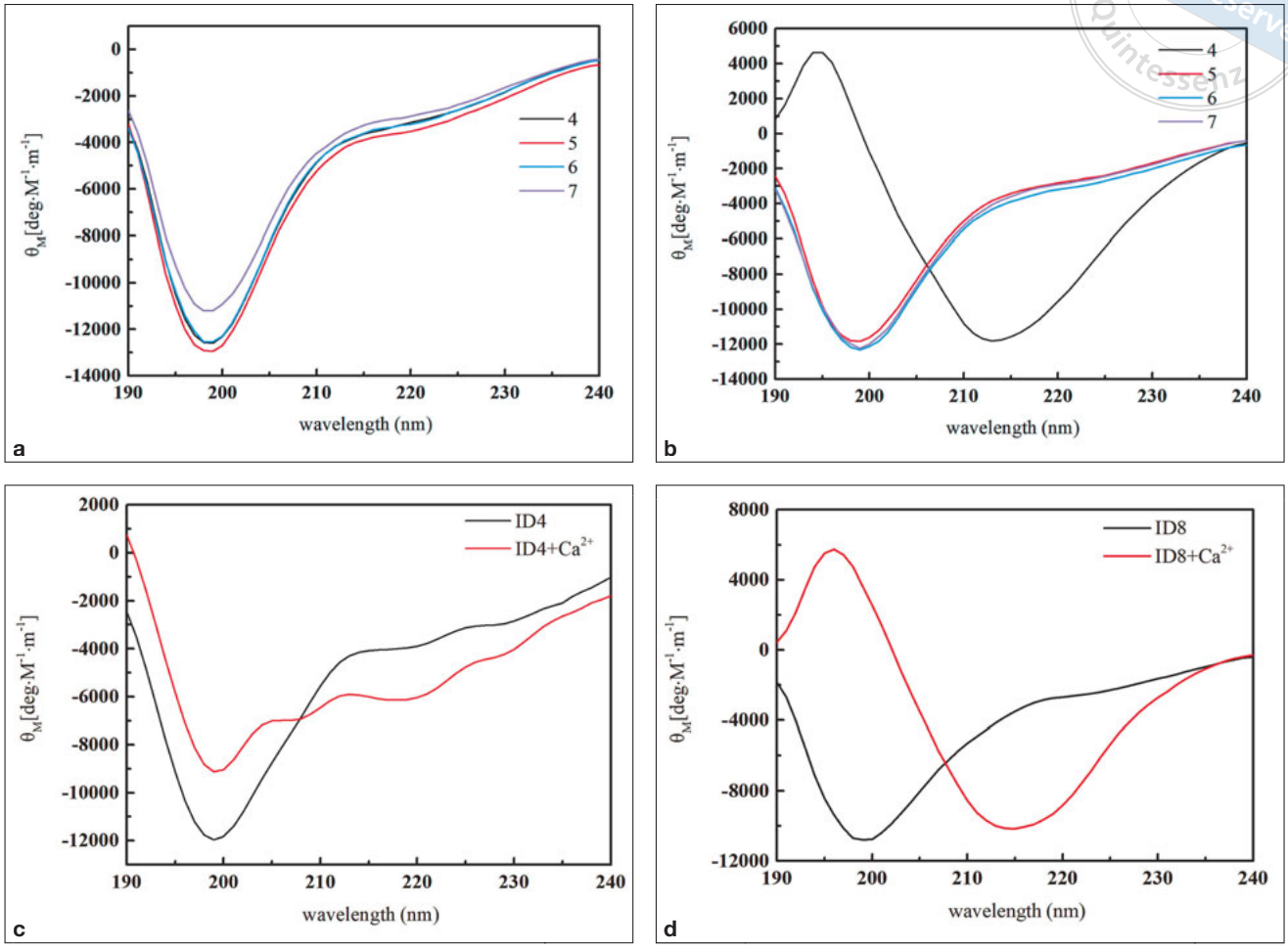

Fig 1 CD of ID4 and ID8. **(a)** CD spectra of ID4 at different pH conditions. **(b)** CD spectra of ID8 at different pH conditions. **(c)** CD spectra of ID4 in the presence and absence of Ca^{2+}. **(d)** CD spectra of ID4 in the presence and absence of Ca^{2+}.

ID4 and ID8 hydrogels promote HAP mineralisation in vitro

SEM images (Figs 5a to 5d) showed that both ID4 and ID8 hydrogel could induce HAP mineralisation. The crystals in the ID4 group exhibited a lower degree of crystallinity, while those in the ID8 group appeared as flower-like, with a higher degree of crystallinity.

TEM with SAED images (Figs 5e to 5h) was consistent with HAP formation. The results showed that the ID4 samples appeared amorphous with a diameter of about 200 nm, while SAED images were consistent with the formation of amorphous calcium phosphate with a lower degree of crystallinity. In the ID8 group, TEM images showed that the crystals appeared as plate-like and exhibited higher crystallinity, while SAED images were consistent with the formation of plate-like HAP crystals, as indicated by the arc patterns at 002 and 211 positions.

XRD results (Figs 6a and 6b) of ID4 showed broad peaks around 2θ = 25 at 1, 4 and 7 days, while ID8 showed sharp peaks at 2θ = 25.8 (002) and 2θ = 31.6 (211) at 4 and 7 days.

In situ remineralisation of initial enamel caries regulated by ID8

After demineralisation, the SMH (Fig 7a) of all samples decreased to 170 KHN and no significant differences were observed between any groups ($P > 0.05$). After 7 days of remineralisation, there was no significant difference in SMH between the DIW group and the etched enamel samples ($P > 0.05$). The SMHR% (Fig 7b) of the NaF and ID8 groups was significantly higher than that of the ID4 and DIW groups ($P < 0.05$), and there was no statistical difference between the ID8 and NaF groups ($P > 0.05$). The XRD patterns (Fig 8a) of etched enamel

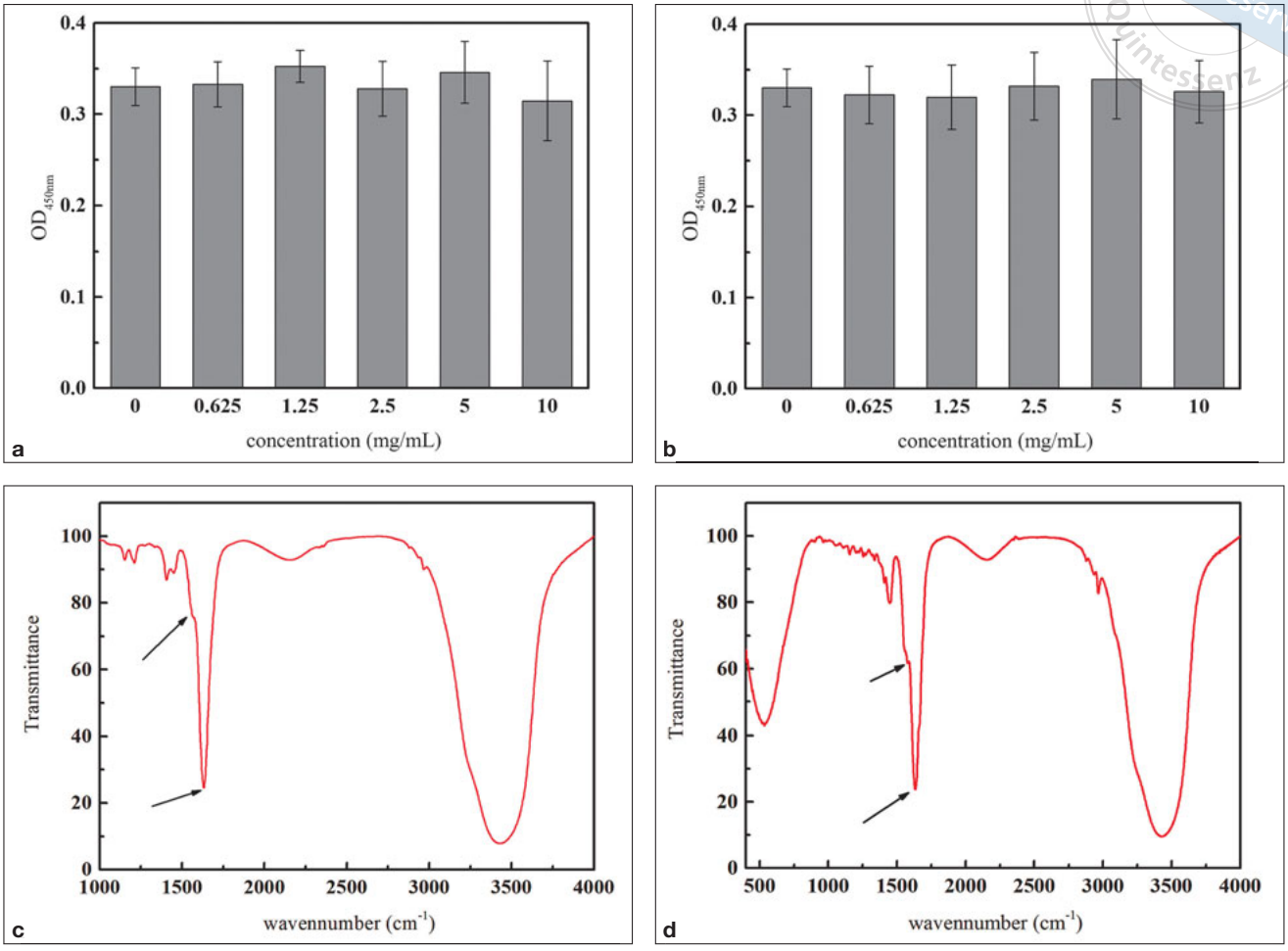

Fig 2 Cell viability analysis and FTIR spectra of ID4 and ID8. **(a)** Effect of HOK cell viability of ID4 at various concentrations determined by CCK-8 assay. **(b)** Effect of HOK cell viability of ID8 at various concentrations determined by CCK-8 assay. **(c)** FTIR spectra of ID4; peaks at 1631 cm^{-1} belong to the amide I band and those at 1565 cm^{-1} belong to the amide II band. **(d)** FTIR spectra of ID8; peaks at 1633 cm^{-1} belong to the amide I band and those at 1558 cm^{-1} belong to the amide II band. These peaks confirmed the β-sheet structure of ID4 and ID8.

were measured for comparison. After remineralisation, the 002 and 211 peaks were significantly enhanced compared with etched enamel, and the sharp peaks of 002 could be seen in both ID4 and ID8 groups.

The mineral loss and lesion depth after treatment were highest in the DIW group, and lower in the ID4, ID8 and NaF groups. Fig 8b exhibits more detailed information about the mineral content at different depths after remineralisation for all groups. All samples in the different groups showed similar mineral composition in the region extending from the enamel surface to a depth of 20 μm. Samples treated with NaF, ID4 and ID8 showed significantly more mineral content than those in the DIW group from the depths of 30 μm to 120 μm, corresponding to the lesion. However, at all the depths examined, the ID8 group showed a greater mineral content than the ID4 and DIW samples. The mineral content in all the groups was similar at depths beyond 130 μm.

Discussion

In this study, the β-sheet peptides ID4 and ID8 with shorter and optimised sequence patterns were designed and synthesised rationally. Both formed hydrogels in the presence of calcium and showed calcium-responsive self-assembly and good stability under neutral physiological conditions. ID4 and ID8 hydrogels could serve as the template to induce HAP nucleation and promote biomimetic remineralisation of initial caries lesions.

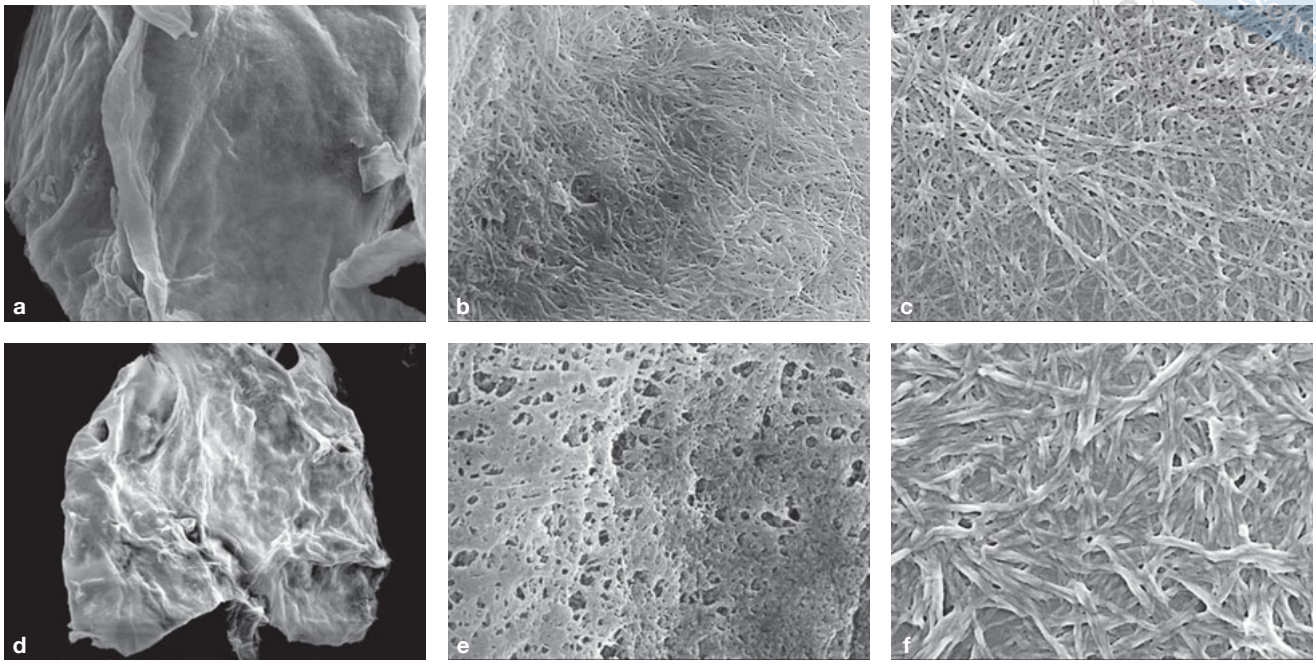

Fig 3 SEM images of self-assembly ID4 and ID8 hydrogel. **(a)–(c)** ID4; **(d)–(f)** ID8. Both ID4 and ID8 self-assembled into nanofibres, and these nanofibres interweaved to form membrane-like structures.

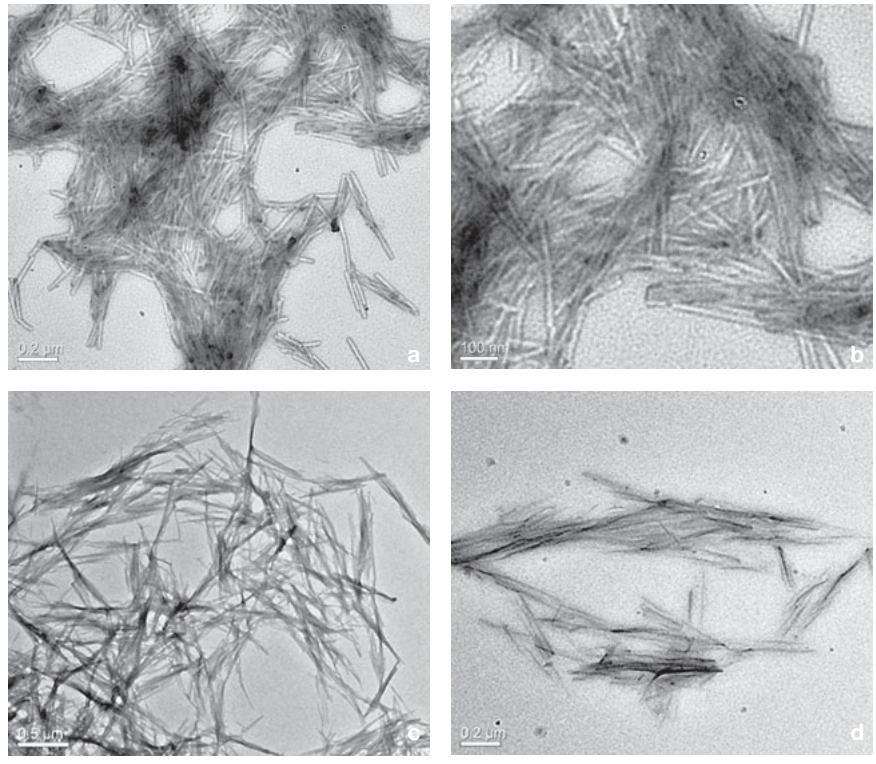

Fig 4 TEM images of self-assembly ID4 and ID8. **(a)** and **(b)** ID4; ID4 nanofibres were about 20 nm in diameter with a length between 0.4 and 0.6 μm. **(c)** and **(d)** ID8; ID8 nanofibres were about 50 nm in diameter with a length between 0.8 and 1.2 μm.

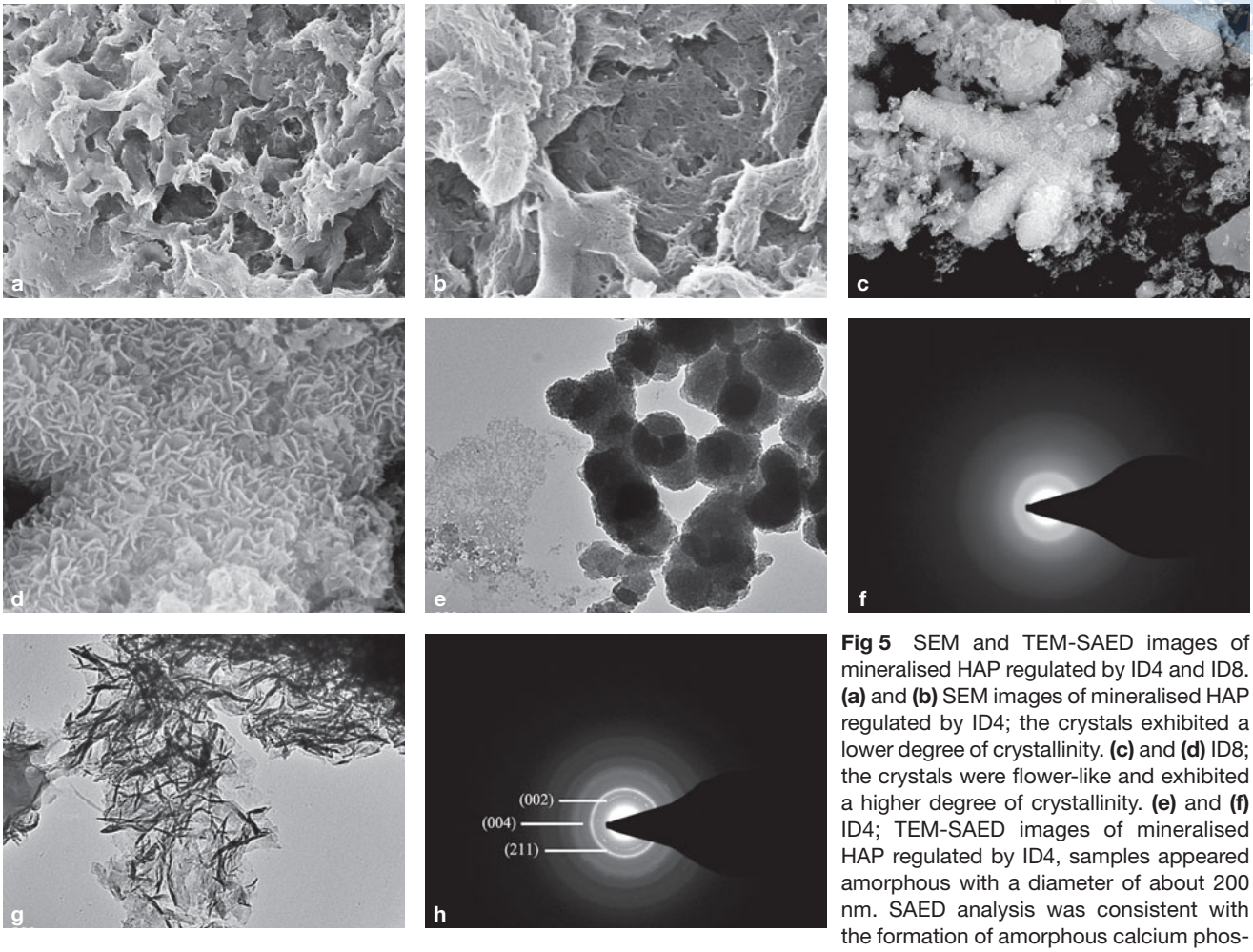

Fig 5 SEM and TEM-SAED images of mineralised HAP regulated by ID4 and ID8. **(a)** and **(b)** SEM images of mineralised HAP regulated by ID4; the crystals exhibited a lower degree of crystallinity. **(c)** and **(d)** ID8; the crystals were flower-like and exhibited a higher degree of crystallinity. **(e)** and **(f)** ID4; TEM-SAED images of mineralised HAP regulated by ID4, samples appeared amorphous with a diameter of about 200 nm. SAED analysis was consistent with the formation of amorphous calcium phosphate. **(g)** and **(h)** TEM-SAED images of mineralised HAP regulated by ID8, samples appeared plate-like and exhibited a higher degree of crystallinity. SAED analyses were consistent with the formation of plate-like HAP crystals, as indicated by the arc patterns at 002 and 211 positions.

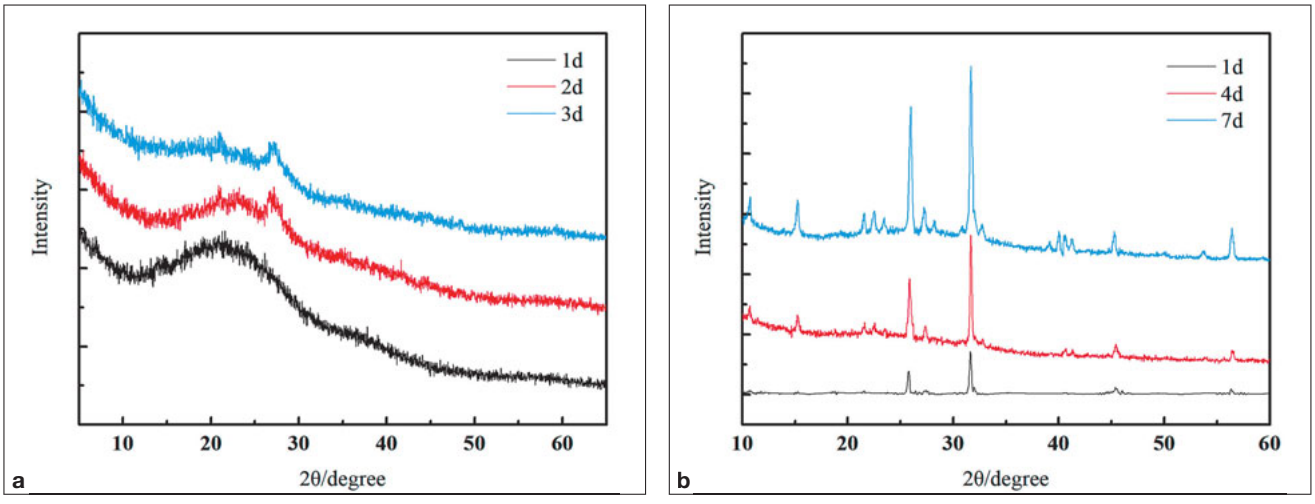

Fig 6 XRD spectra of mineralised ID4 and ID8 hydrogel. **(a)** XRD spectra of mineralised ID4 hydrogel; broad peaks could be seen around 2θ = 25 at 1, 4 and 7 days. **(b)** XRD spectra of mineralised ID8 hydrogel; sharp peaks could be seen at 2θ = 25.8 (002) and 2θ = 31.6 (211) at 4 and 7 days.

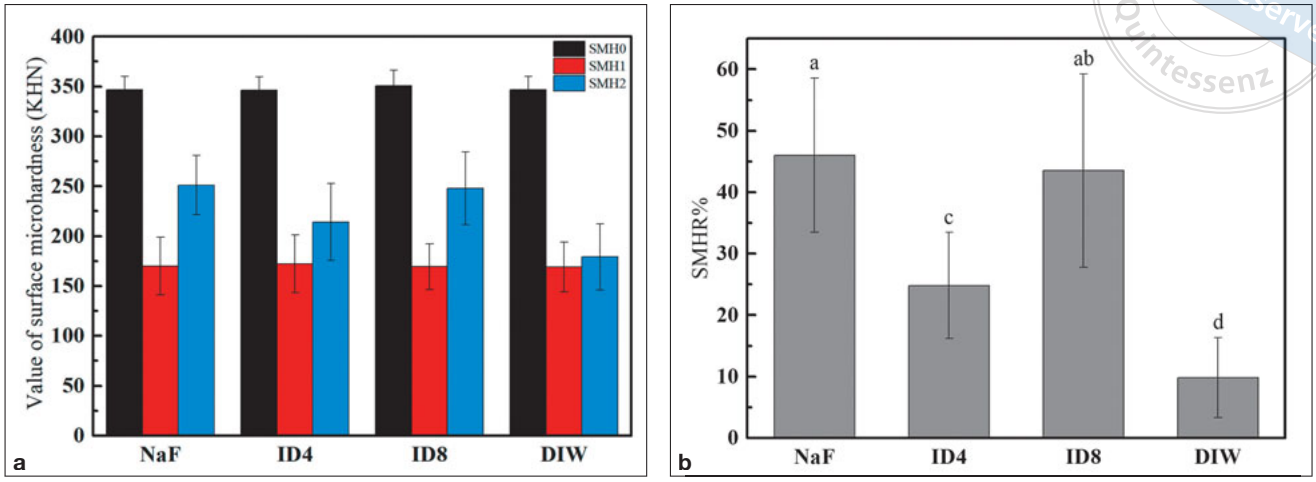

Fig 7 SMH analysis of the enamel samples in the remineralisation assay. **(a)** SMH of the NaF group, ID4-treated group, ID8-treated group and DIW group before etching, after etching and after remineralisation. **(b)** SMHR% of the NaF group, ID4-treated group, ID8-treated group and DIW group after being immersed in artificial saliva for 7 days. The statistical analysis was performed using ANOVA followed by a Student paired t test. In each plot, dissimilar letters indicate significantly different values ($P < 0.05$).

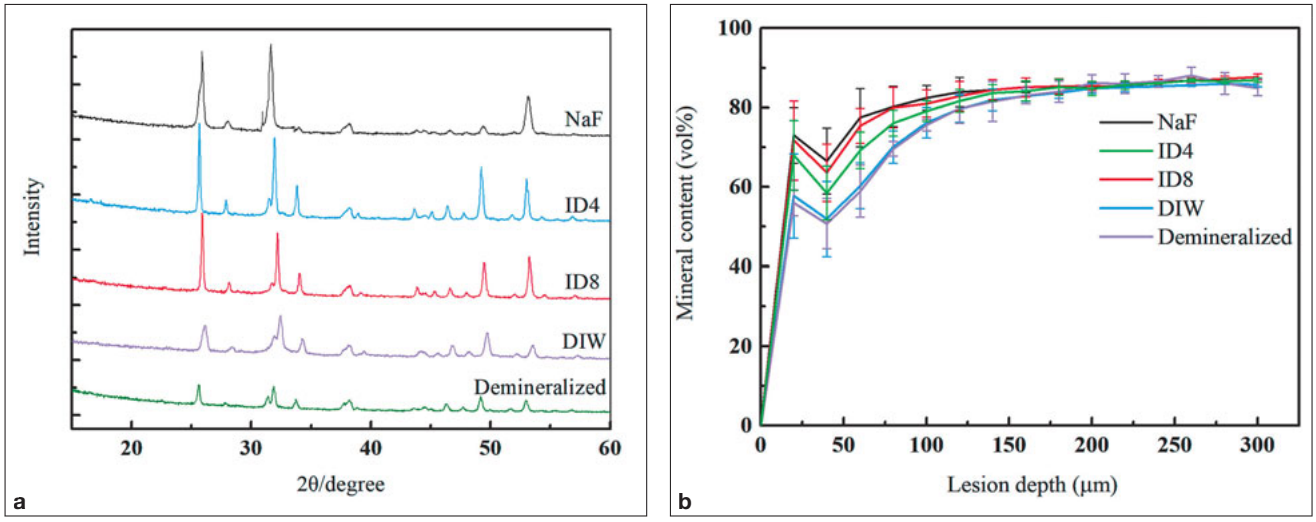

Fig 8 XRD spectra and TMR analysis of the enamel samples in the remineralisation assay. **(a)** XRD spectra after remineralisation treatment in the presence of NaF, ID4, ID8 or DIW alone. **(b)** TMR analysis of enamel sections before and after remineralisation treatment in the presence of NaF, ID4, ID8 or DIW alone. The results showed mineral content (vol% μm) vs. depth (μm) for lesions.

Compared with ID4, ID8 showed better efficacy; this was thought to be related to its higher β-sheet content. These results indicated that ID8 could be a promising bioactive component for anti-caries application.

Synthetic peptides have been widely applied to biomimetic mineralisation of bone and teeth. In general, several types of synthetic peptides have been utilised in biomimetic processes for hard tissue remineralisation. Type I are proteins or peptides that take part in biomineralisation, such as amelogenin, amelotin, dentine matrix protein-1, statherin and elastin[2,4,23,24]; type II are proteins or peptides inspired by proteins in biomineralisation, with sequence patterns that are usually the functional regions of biomacromolecules, such as LRAP, the peptides P26 and P32, P11-4, QP5 and DE-11[2,3,5,6,8,10]; and type III are de novo synthetic peptides, such as P_{FD}-5 and Z1[9,20]. Compared with type I and type II peptides, de novo synthetic peptides can now be programmed to self-assemble into predefined conformations and nanostructures. However, classic ionic self-complementary self-assembly β-sheet peptides employed long sequence patterns and were not

stable enough under physiological conditions, therefore the β-sheet peptides ID4 and ID8 with shorter and optimised sequence patterns were designed and synthesised rationally in this report. Both were de novo synthetic classic ionic self-complementary self-assembly β-sheet peptides, and also proved to be stable under neutral physiological conditions.

In this report, RP-HPLC and mass spectra results confirmed the successful synthesis of ID4 and ID8. A cell proliferation assay proved that both ID4 and ID8 showed low cytotoxicity. Their self-assembly capability was also explored. Molecular self-assembly is a spontaneous organisation of molecules under thermodynamic equilibrium conditions through noncovalent interactions. These noncovalent interactions include hydrogen bonds, ionic bonds and van der Waals bonds. Although each of the bonds is rather weak, their combination can result in very stable structures. Therefore, the pH of the solution and the addition of alkaline cations will significantly influence the noncovalent interactions in the solution and then influence the self-assembly of peptides. In this study, the pH of the solution and whether it contained calcium ions or not were selected as two environmental conditions of peptide self-assembly. CD measurements showed that the percentage of β-sheet in ID4 increased to 52.6% from 20.3% in the presence of Ca^{2+} under a neutral pH environment. ID8 was unstructured at pH 5.0, 6.0 and 7.0 while self-assembled into β-sheet at pH 4,0 and could self-assemble into β-sheet in the presence of Ca^{2+} in a neutral pH environment. These results indicated the calcium-responsive self-assembly of ID4 and ID8. At the same time, calcium could induce the self-assembly of transparent ID4 and ID8 hydrogels. FTIR results confirmed the β-sheet structure of ID8 hydrogel. SEM and TEM images provided visualised self-assembly nanofibres of ID4 and ID8 hydrogels, and the nanofibres of ID8 were larger. SEM and TEM images also showed that both ID4 and ID8 hydrogels induced HAP mineralisation, the crystals in the ID4 group exhibited a lower degree of crystallinity, while the crystals in the ID8 group appeared as flower-like and with a higher degree of crystallinity. TEM with SAED images showed that the ID4 samples appeared amorphous with a diameter of about 200 nm. SAED images were consistent with the formation of amorphous calcium phosphate with a lower degree of crystallinity. In the ID8 group, TEM images showed that the crystals appeared as plate-like and exhibited higher crystallinity, while SAED images were consistent with the formation of plate-like HAP crystals, as indicated by the arc patterns at 002 and 211 positions.

We also developed an in situ remineralisation experiment. All groups achieved varying degrees of remineralisation when compared with that of the DIW group. The results of SMHR% showed that the NaF group had the highest hardness recovery rate, followed by ID8, and there was no significant difference between the ID8 and NaF groups ($P < 0.05$). Of all the groups examined, ID8 and NaF groups showed a higher SMHR%. In the XRD results, the 002 and 211 peaks were significantly enhanced compared with etched enamel, and the sharp 002 peaks could be seen in both the ID4 and ID8 groups, indicating that the orientation of crystal growth was along the c-axis. As the gold standard technique, TMR was then performed to quantitate the remineralisation of enamel. The results showed that mineral loss, lesion depth and mineral content of the surface layer and lesion body after 7 days of remineralisation were similar in the samples treated with ID8 and NaF, which presented a higher mineral content than the ID4 and DIW groups. Combined with the results of SMHR%, we concluded that remineralisation by the ID8 group was closer to that of natural enamel compared with ID4.

The potential mechanism of ID8 hydrogel in promoting remineralisation of initial caries lesions was also explored. HAP belongs to the $P6_3$ space group with the lattice parameters of a = b = 9.432 Å, c = 6.881 Å; meanwhile, the distance between adjacent peptide chains in β-sheet structure is about 4.7–4.8 Å, which is half the length of the a-axis and b-axis; the pivot distance between every two amino acid residues in peptide chains of β-sheet structure is approximately 6.9 Å, the same as the length of the c-axis[9]. Lattice matching can effectively reduce the activation energy of HAP nucleation. In addition, β-sheet peptide self-assembling into nanofibre scaffolds could regulate the growth and arrangement of HAP crystals. Our research group previously designed and synthesised a peptide based on amelogenin named QP5, which is a 22-residue peptide consisting of five tandem amelogenin (Gln-Pro-X) repeats followed by a 7-residue hydrophilic tail; the remineralisation effect of QP5 was confirmed by our previous studies[1,6,10]. The β-sheet of QP5 is thought to be related to its promotion of remineralisation while it merely contains 36.1% of β-sheet. It is possible to obtain a better remineralisation effect by designing a peptide with a higher content of β-sheet structure[1,6,9,10,22,25]. In this study, the β-sheet peptides ID4 and ID8 with shorter and optimised sequence patterns were designed rationally, the percentage of β-sheet in ID4 increased to 52.6% and ID8 contained a total of 99.63% β-sheet, which is thought to be the reason why ID8 showed better remineralisation efficacy.

Conclusion

In this study, the β-sheet peptides ID4 and ID8 with shorter and optimised sequence patterns were designed and synthesised rationally. Both showed calcium-responsive self-assembly and ID8 contained a total of 99.63% β-sheet. ID4 and ID8 hydrogels could serve as the template to induce HAP nucleation and promote biomimetic remineralisation of initial caries lesions. ID8 showed better efficacy than ID4, and this was thought to be related to its higher β-sheet content. These results underpin future research on peptide design and ID8 may be a promising bioactive component for anti-caries application. Meanwhile, more systematic experiments are necessary to verify the efficacy of ID8.

Conflicts of interest

The authors declare no conflicts of interest related to this study.

Author contribution

Drs Zhong Cheng LI and Qin XI contributed to the work equally, conducted the experiments and participated in drafting the manuscript; Drs Qian REN, Die HU, Tian TIAN and Ting HE participated in preparing the samples; Dr Wei LI revised the manuscript; Dr Ling Lin ZHANG designed the study and revised the manuscript.

(Received Nov 25, 2019; accepted Dec 16, 2019)

References

1. Ren Q, Ding L, Li Z, et al. Chitosan hydrogel containing amelogenin-derived peptide: Inhibition of cariogenic bacteria and promotion of remineralization of initial caries lesions. Arch Oral Biol 2019;100:42–48.
2. Wang K, Wang X, Li H, et al. A statherin-derived peptide promotes hydroxyapatite crystallization and in situ remineralization of artificial enamel caries. RSC Adv 2018;8:1647–1655.
3. Le Norcy E, Kwak SY, Wiedemann-Bidlack FB, et al. Leucine-rich amelogenin peptides regulate mineralization in vitro. J Dent Res 2011; 90:1091–1097.
4. Zhou Y, Zhou Y, Gao L, Wu C, Chang J. Synthesis of artificial dental enamel by an elastin-like polypeptide assisted biomimetic approach. J Mater Chem B 2018;6:844–853.
5. Mukherjee K, Ruan Q, Nutt S, Tao J, De Yoreo JJ, Moradian-Oldak J. Peptide-based bioinspired approach to regrowing multilayered aprismatic enamel. ACS Omega 2018;3:2546–2557.
6. Li D, Lv X, Tu H, Zhou X, Yu H, Zhang L. Remineralization of initial enamel caries in vitro using a novel peptide based on amelogenin. Front. Mater. Sci. 2015;9:293–302.
7. Kwak SY, Litman A, Margolis HC, Yamakoshi Y, Simmer JP. Biomimetic enamel regeneration mediated by leucine-rich amelogenin peptide. J Dent Res 2017;96:524–530.
8. Alkilzy M, Tarabaih A, Santamaria RM, Splieth CH. Self-assembling peptide P11-4 and fluoride for regenerating enamel. J Dent Res 2018;97:148–154.
9. Segman-Magidovich S, Grisaru H, Gitli T, Levi-Kalisman Y, Rapaport H. Matrices of acidic β-sheet peptides as templates for calcium phosphate mineralization. Advanced Materials 2008;20:2156–2161.
10. Lv X, Yang Y, Han S, et al. Potential of an amelogenin based peptide in promoting remineralization of initial enamel caries. Arch Oral Biol 2015;60:1482–1487.
11. Ruan Q, Moradian-Oldak J. Amelogenin and enamel biomimetics. J Mater Chem B 2015;3:3112–3129.
12. Ren D, Ruan Q, Tao J, Lo J, Nutt S, Moradian-Oldak J. Amelogenin affects brushite crystal morphology and promotes its phase transformation to monetite. Cryst Growth Des 2016;16:4981–4990.
13. Li QL, Ning TY, Cao Y, Zhang WB, Mei ML, Chu CH. A novel self-assembled oligopeptide amphiphile for biomimetic mineralization of enamel. BMC Biotechnol 2014;14:32.
14. Hartgerink JD, Beniash E, Stupp SI. Self-assembly and mineralization of peptide-amphiphile nanofibers. Science 2001;294:1684–1688.
15. Aggeli A, Nyrkova IA, Bell M, et al. Hierarchical self-assembly of chiral rod-like molecules as a model for peptide beta -sheet tapes, ribbons, fibrils, and fibers. Proc Natl Acad Sci U S A 2001;98:11857–11862.
16. Acar H, Srivastava S, Chung EJ, et al. Self-assembling peptide-based building blocks in medical applications. Adv Drug Deliv Rev 2017;110–111:65–79.
17. Abbas M, Zou Q, Li S, Yan X. Self-assembled peptide- and protein-based nanomaterials for antitumor photodynamic and photothermal therapy [epub 6 January 2017]. Adv Mater 2017;29. doi: 10.1002/adma.201605021.
18. He G, Dahl T, Veis A, George A. Nucleation of apatite crystals in vitro by self-assembled dentin matrix protein 1. Nat Mater 2003;2:552–558.
19. Stendahl JC, Rao MS, Guler MO, Stupp SI. Intermolecular forces in the self-assembly of peptide amphiphile nanofibers. Advanced Functional Materials 2006;16:499–508.
20. Zhang H, Park J, Jiang Y, Woodrow KA. Rational design of charged peptides that self-assemble into robust nanofibers as immune-functional scaffolds. Acta Biomater 2017;55:183–193.
21. Semino CE. Self-assembling peptides: from bio-inspired materials to bone regeneration. J Dent Res 2008;87:606–616.
22. Saiani A, Mohammed A, Frielinghaus H, et al. Self-assembly and gelation properties of α-helix versus β-sheet forming peptides. Soft Matter 2009;5:193–202.
23. Abbarin N, San Miguel S, Holcroft J, Iwasaki K, Ganss B. The enamel protein amelotin is a promoter of hydroxyapatite mineralization. J Bone Miner Res 2015;30:775–785.
24. Ruan Q, Zhang Y, Yang X, Nutt S, Moradian-Oldak J. An amelogenin-chitosan matrix promotes assembly of an enamel-like layer with a dense interface. Acta Biomater 2013;9:7289–7297.
25. Zhang S. Emerging biological materials through molecular self-assembly. Biotechnol Adv 2002;20:321–339.